JET PROPULSION LABORATORY INTEROFFICE MEMORANDUM

352J-97-008

January 9, 1997

TO: G. Blackwood

FROM: L. Jandura

SUBJECT: SIM Optical Performance Metric for Optical Pathlength Difference

SUMMARY:

This memo defines the optical performance metric for optical pathlength difference (OPD) used to evaluate the SIM instrument performance in the presence of reaction wheel disturbances. This single scalar metric quantifies the interference fringe blur on the CCD detector as a function of coherent integration time, closed loop bandwidths for the delay line servo and fringe tracker, structural transmission of reaction wheel disturbances, and the instrument operating mode (fringe acquisition or fringe tracking). The metric defined in this memo will be used in future analyses to determine isolation requirements for SIM. In addition this memo describes the operating modes to be evaluated with the performance metric, the equations needed to perform the evaluation, and their corresponding performance requirements.

Distribution:

M. Colavita
R. Grogan
B. Hines
S. Joshi
R. Laskin
M. Levine-West
G. Lilienthal
T. Livermore
W. Mateer
J. Melody
M. Milman
G. Neat
Z. Rahman
M. Shao
J. Spanos
R. Stoller
J. Umland
J. Yu

Introduction

As part of the Space Interferometer Mission (SIM) and the Interferometry Technology Program (ITP), work is underway to determine what level of vibration isolation is required to enable SIM to perform its science mission in the presence of disturbances from the reaction wheels on the SIM spacecraft. This effort is part of a larger modeling and analysis effort designed to evaluate the effectiveness of all the layered vibration control technologies: active optical control, structural quieting, and vibration isolation.

This memo describes the optical performance metric for optical pathlength difference (OPD) needed to link the output of the SIM integrated models to the desired science requirements for the cases particularly relevant to vibration isolation of the reaction wheel disturbance. More complete documentation of the vibration isolation modeling effort and the associated vibration isolation requirements is found in two working documents, Vibration Isolation Subsystem, SIM Modeling Document and Vibration Isolation Subsystem, Brassboard Hardware Document [6, 7].

Functions and Operating Modes of SIM

SIM is a free-flying optical interferometer with four different types of scientific objectives: wide-angle astrometry, narrow-angle astrometry, rotational synthesis imaging, and interferometric fringe nulling. In terms of the spacecraft and instrument operation, these are called Instrument Functions and are referred to as:

- Astrometry (wide-angle)
- Astrometry (narrow-angle)
- Imaging
- Nulling

Each Instrument Function is composed of Instrument Modes of Operation (or Instrument Modes) as illustrated in Figure 1. Instrument Modes are defined as jobs the three-baseline instrument must accomplish to perform the Instrument Function. For instance, *Wavefront Tilt (WFT) Acquisition* is the first Instrument Mode that must be performed to meet the Instrument Function of *Astrometry*. Instrument Modes themselves are further decomposed into Interferometer Modes of Operation (or Interferometer Modes) which are tasks that a single baseline interferometer must perform to enable an Instrument Mode to take place. *Guide Fringe Acquisition* is the Interferometer Mode needed to accomplish the Instrument Mode of *Guide Star Fringe Acquisition*. This process can only proceed if a physical motion requirement on the rate of fringe motion is met. Figure 1 outlines all

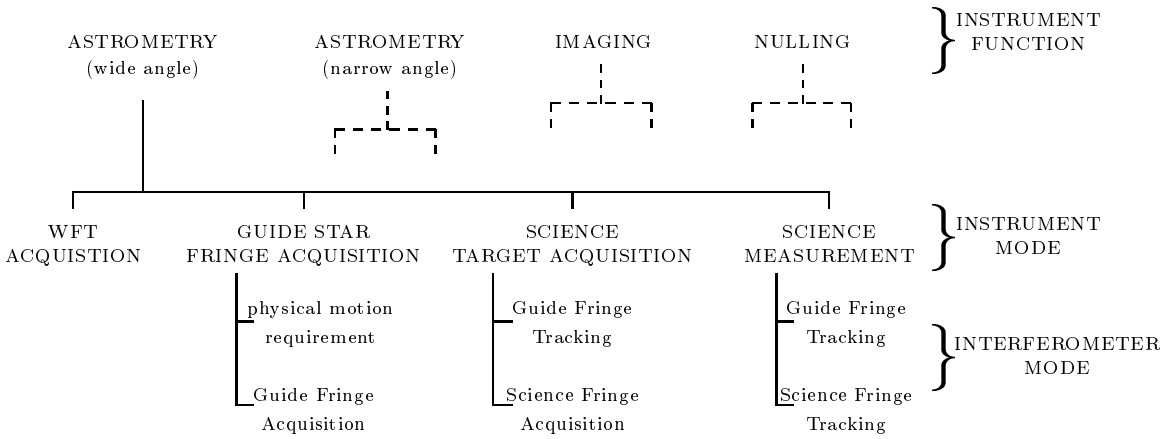

Figure 1: Overview of instrument functions, instrument modes and interferometer modes for SIM.

Instrument Modes and Interferometer Modes for the wide-angle astrometry Instrument Function.

During Wavefront Tilt (WFT) Acquisition, each baseline first must acquire a wavefront tilt signal from the guide star on the CCD detector. This is accomplished by orienting the spacecraft, moving the siderostats and quasistatically adjusting the fast steering mirror or alignment mirrors until the guide star appears on the CCD detector. These steps are repeated for both arms in each baseline, and for both guide interferometer baselines. When acquisition is complete, high frequency feedback compensation of the wavefront tilt is implemented using the fast steering mirrors.

Each guide interferometer must then acquire the interference fringe of the guide star. A necessary condition for the success of the fringe hunt is that the rate of fringe motion (physical motion as seen at the CCD detector array) must be less than the search rate of the delay line. This condition poses a priori limits on the maximum fringe OPD dynamic error due to structural disturbances. A second necessary condition for fringe acquisition is that the high frequency jitter (blur) of OPD during the coherent integration time, T_c must be less than $\lambda/10$; if not, the fringe cannot be resolved.

After successful fringe acquisition the fringe tracker loop can be closed at a bandwidth of 1/10 of the sampling frequency or approximately $0.1/T_c\ Hz$ on each guide interferometer. T_c is typically *1 millisecond* making the control bandwidth 100 Hz. The fringe tracker loop may help to reduce the OPD jitter on the detector during T_c; to be useful as a feedforward signal to the guide interferometer, this OPD jitter must be less than $\lambda/20$. With feedforward from both guide star baselines within the stated error budget,

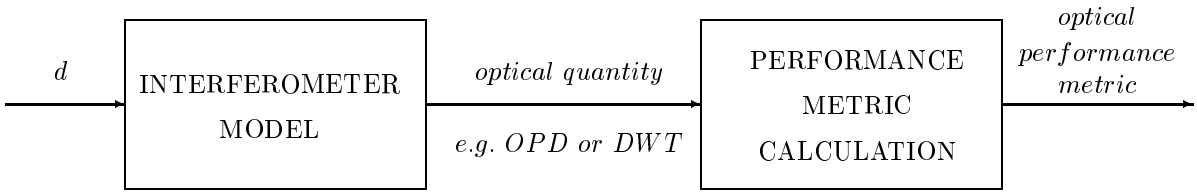

Figure 2: Overview of the disturbance analysis method.

the science interferometer can acquire the science target and close low-frequency (0.1 or 1 Hz) fringe tracking loops on the science target.

In previous work [3, 4] for the SITE and ISIS projects, emphasis was placed on defining metrics for fringe acquisition and fringe tracking of the guide interferometer. These operating modes are the most relevant for the reaction wheel disturbance analysis for OPD errors because the performance requirements for OPD fringe blur are written such that meeting the requirements for these two Guide Interferometer Modes enables the Science Interferometer to perform at the desired level. The following sections define the two Guide Interferometer Modes for SIM, *Guide Interferometer Fringe Acquisition and Guide Interferometer Fringe Tracking*, which will just be called *Fringe Acquisition and Fringe Tracking* in later sections. Also presented are the optical performance metric of fringe blur and the corresponding performance requirements that must be met with each operating mode.

Operating Modes, Performance Metric, and Requirements

Figure 2 describes the general method used to analyze a reaction wheel disturbance problem. The disturbance source, d, is injected into a model of a particular operating mode of the interferometer. The output of this model is a time or frequency based description of one or more optical quantities such as optical pathlength difference (OPD) or differential wavefront tilt (DWT) that are relevant to interferometer operation. This description is processed further by a mathematical statement, the performance metric calculation, which relates the optical quantity to a specific performance characteristic of the interferometer. The output of this process is a specific value of an optical performance metric which can then be compared to the corresponding performance requirement describing successful interferometer operation.

The interferometer model is a set of transfer functions that relate the effect of each

disturbance force and torque on each optical quantity. The effects of the multiple disturbance forces and torques produced by a single reaction wheel are handled using linear superposition. Multiple reaction wheels are analyzed using the same technique.

The interferometer model is composed of a structural model, an optical model and a control loop model. The structural and optical model are the same for all the operating modes while the control loop model changes with the operating modes. An operating mode can be expressed in control block diagram form with specific parameters and loops closed. Both Instrument Modes (multiple baselines) and Interferometer Modes can be considered by the use of an appropriate model.

SIM Operating Modes

Figure 3 is a block diagram of the open-loop interferometer model. A reaction wheel force disturbance, d, drives a structural-optical model of the spacecraft instrument, G_p, to produce physical pathlength output, y_{opd}. y_{opd} is the difference in pathlength, measured between a common wavefront external to the instrument and the beam combiner, traveled by light that enters at the two separate collecting apertures of the interferometer baseline. y_{opd} is represented as the sum of pathlength differences internal to the instrument, y_i (between the beam combiner and the collecting apertures) and pathlength differences external to the instrument, y_e (between the common wavefront and the collecting apertures). Either quantity may be quasistatic or dynamic.

The reaction wheel disturbance, d, in the block diagram represents a disturbance force (or torque) in only a single direction. Likewise, the transfer function of the structural plant, G_p, maps the contribution of that particular force or torque direction to the total OPD error. Since a reaction wheel contains disturbances in three force directions and two torque directions, the contributions of all these disturbances to the total OPD error is determined using linear superposition. The use of linear superposition requires the assumption that the input disturbances are uncorrelated, random disturbances. Although this assumption is not true for the reaction wheel disturbances, its use provides a conservative estimate of the total OPD error and therefore will be tolerated for this analysis. The analysis described in this memo is done in the frequency domain. $\Phi_{y_{OPD}}(w)$, the autospectrum of y_{opd} is related to $\Phi_{dj}(w)$, the autospectrum of a disturbance force or torque in a particular direction by

$$\Phi_{y_{OPD}}(w) = \sum_{j=1}^{n} |G_{pj}(\omega)|^2 \, \Phi_{dj}(w) \tag{1}$$

where $G_{pj}(\omega)$ is the transfer function of the structural plant relating the particular disturbance force or torque to OPD error. The total OPD error is the summation of the contribution of all force or torque components from all reaction wheels considered in the

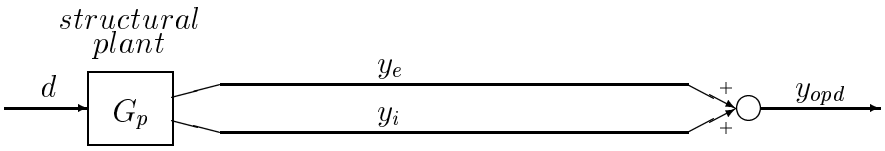

Figure 3: Block diagram of the open-loop interferometer model.

analysis.

In the sections that follow, additional blocks will be added to the open-loop interferometer model to represent the control action for the fringe acquisition and fringe tracking operating modes. Both OPD and WFT are optical output quantities of interest but only OPD will be considered here. Disturbance effects on WFT are considered in another memo by J. Melody [5].

Fringe Acquistion

Figure 4 illustrates a block diagram of the interferometer model for the Fringe Acquisition operating mode. In this operating mode the only control loop closed is the delay line control system. The reaction wheel disturbance, d, enters the integrated structure and optics model represented by G_p. The output of this model is split up into internal and external OPD, y_i and y_e. The internal OPD is assumed to be perfectly sensed by the internal metrology system and corrected by the optical delay line, represented here by its open loop plant, G_d and its compensator, K_d. Whatever internal OPD remains uncorrected is added to the uncorrected external OPD to produce the desired optical output quantity, stellar OPD or y_{opd}.

Now $\Phi_{y_{OPD}}(w)$, the autospectrum of y_{opd} is related to $\Phi_{dj}(w)$, the autospectrum of a disturbance force or torque in a particular direction by

$$\Phi_{y_{OPD}}(w) = \sum_{j=1}^{n} \left| [G_{pj}(\omega)]_e + S_d [G_{pj}(\omega)]_i \right|^2 \Phi_{dj}(w) \tag{2}$$

where $[G_{pj}(\omega)]_e$ is the transfer function of the structural plant relating the particular disturbance force or torque to external OPD error, $[G_{pj}(\omega)]_i$ is the transfer function of the structural plant relating the particular disturbance force or torque to internal OPD error, and S_d is the sensitivity function of the delay line as shown in the simplified block diagram of Figure 5.

$$S_d = \frac{1}{1 + K_d G_d} \tag{3}$$

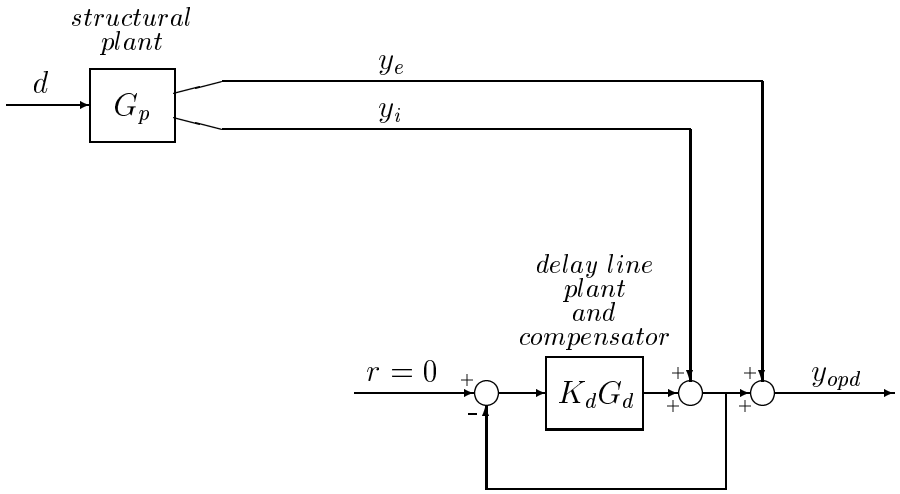

Figure 4: Block diagram of the interferometer model for fringe acquisition with OPD as the optical output quantity.

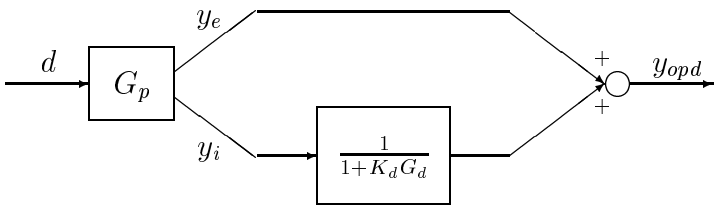

Figure 5: Simplified block diagram of fringe acquisition.

Fringe Tracking

Figure 6 is the block diagram of the interferometer model that illustrates the fringe tracking mode. The structure is identical to that of the aquisition mode with the addition of an additional outer control loop, the fringe tracking loop. Physical OPD, y_{opd}, is measured by the location of an interference fringe on the CCD detector; the fringe displacement on the detector is proportional to y_{opd}. The CCD detector integrates over time T_c and signal m is the sampled mean during the intergration time T_c. The filter H_T is a continuous time approximation of the sampled mean process and is represented by the following equation.

$$H_T(\omega) = sinc\left(\frac{\omega T_c}{2}\right) \tag{4}$$

K_f is the fringe tracker compensator. The output of K_f is r, a servo command for the optical delay line, which will introduce an internal OPD, y_i, to offset the external OPD, y_e over the bandwidth of the delay line control loop.

For this case, $\Phi_{y_{OPD}}(w)$, is related to $\Phi_{dj}(w)$ by

$$\Phi_{y_{OPD}}(w) = \sum_{j=1}^{n} \left|S_f([G_{pj}(\omega)]_e + S_d[G_{pj}(\omega)]_i)\right|^2 \Phi_{dj}(w) \tag{5}$$

where S_f is the closed loop sensitivity function of the fringe tracker loop as shown in the simplified block diagram of Figure 7.

$$S_f = \frac{1}{1 + H_T K_f C_d} \tag{6}$$

where C_d is the complementary sensitivity function of the delay line.

$$C_d = 1 - S_d = \frac{K_d G_d}{1 + K_d G_d} \tag{7}$$

SIM Optical Performance Metric

The performance metric for both the fringe acquisition and fringe tracking modes of the interferometer is the fringe blur on the detector during the coherent integration time, T_c. The amount of blur depends on the stability of both OPD and DWT; only OPD will be considered here. Following the derivation of reference [1], $e_T(\tau, t)$, the OPD error during the integration time T_c is defined as the difference between the continuous time signal $y_{opd}(\tau)$ and its windowed mean, $m(t)$.

$$e_T(\tau, t) = y_{opd}(\tau) - m(t) \qquad t \le \tau \le t + T_c \tag{8}$$

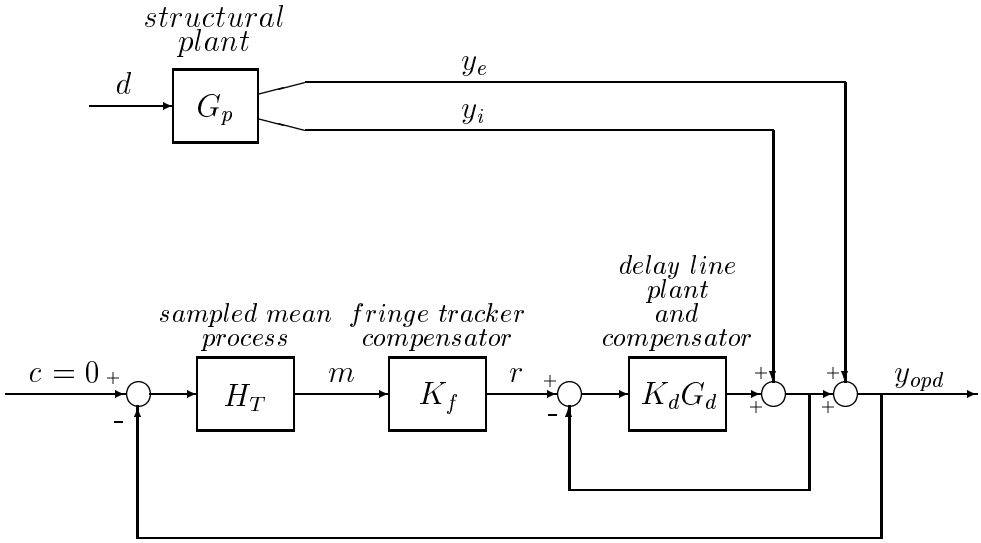

Figure 6: Block diagram of the interferometer model for fringe tracking with OPD as the optical output quantity.

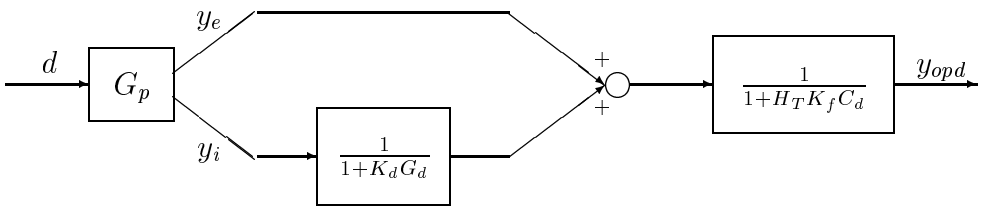

Figure 7: Simplified block diagram of fringe tracking.

$\Phi_{e_T}(w)$, the autospectrum of the OPD error signal is related to $\Phi_{y_{OPD}}(w)$, the autospectrum of y_{opd} by

$$\Phi_{e_T}(w) = |S_T(w)|^2 \, \Phi_{y_{OPD}}(w) \tag{9}$$

where $|S_T(\omega)|^2$ is the high pass filter

$$\begin{aligned} |S_T(\omega)|^2 &= 1 - sinc^2\left(\frac{\omega T_c}{2}\right) &(10)\\ &= 1 - 2\left[\frac{1 - cos(\omega T_c)}{(\omega T_c)^2}\right] &(11)\end{aligned}$$

Signals in y_{opd} which are below the sampling frequency $1/T_c$ are attenuated by this filter; the plot of the filter is shown in Figure 8. The performance metric, σ_{e_T}, is the RMS value of the fringe blur and its value can be directly compared to the requirements presented in the next section. The variance of the fringe blur, $\sigma^2_{e_T}$ is calculated using the following equation.

$$\sigma^2_{e_T} = \frac{1}{2\pi}\int_{-\infty}^{\infty} |S_T(w)|^2 \, \Phi_{y_{OPD}}(w) dw \tag{12}$$

SIM Requirements

In this section the requirements for OPD variation, σ_{OPD}, are derived for the two operating modes, fringe acquisition and fringe tracking. This requirement must be met in the presence of disturbances from all reaction wheels on SIM. For fringe tracking, the OPD and DWT requirements derive from a stellar fringe visibility requirement of 90% for dynamic reductions [2]. Dividing this evenly between DWT and OPD the requirement for the contribution of each is 95% (*i.e.*, $0.9^{\frac{1}{2}}$). During acquisition, the visibility requirement is relaxed to 50% (71% each for DWT and OPD) on the assumption that the fringe can be acquired at half of the signal-to-noise ratio required for tracking. Only the requirement for OPD will be derived here since the OPD metric is the only one considered in this memo.

OPD variation, σ_{OPD} is related to stellar fringe visibility, V using the following equations [2].

$$V = \exp\left\{-\frac{1}{2}\left[2\pi\lambda_{OPD}\right]^2\right\} \tag{13}$$

$$\lambda_{OPD} = \frac{\sigma_{OPD}}{\lambda_0} \tag{14}$$

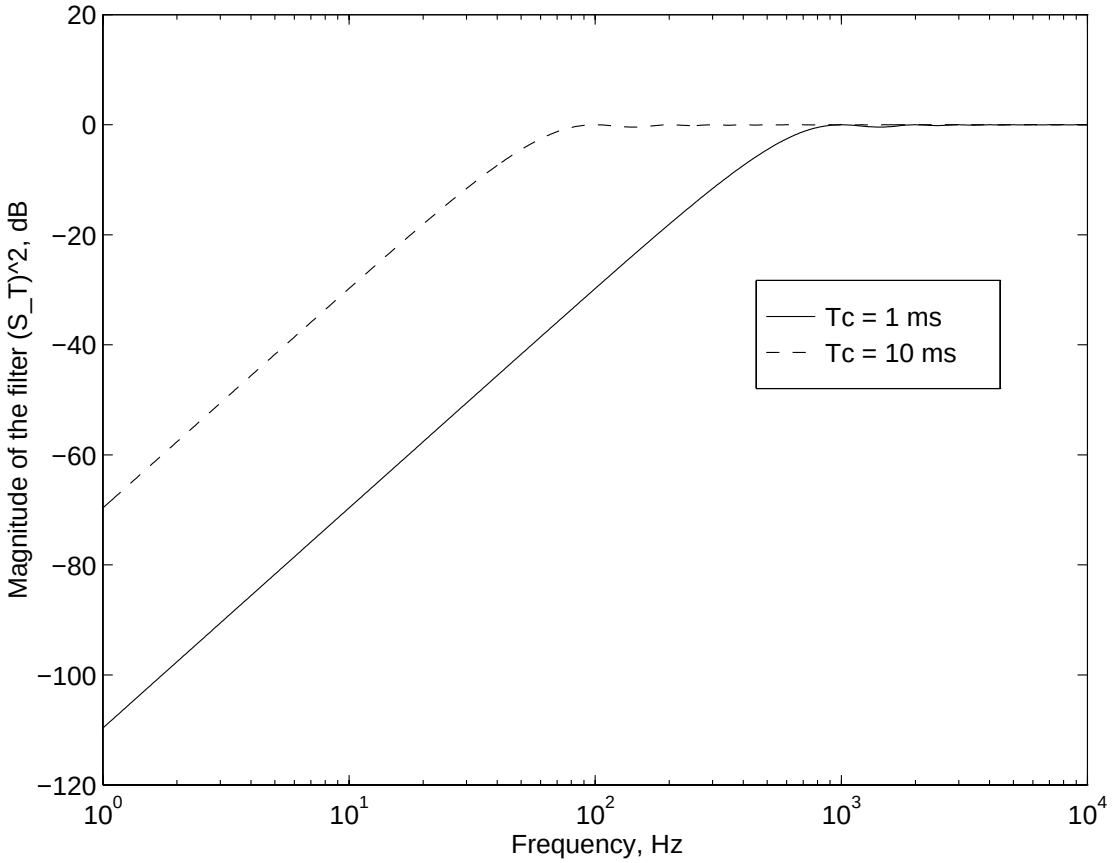

Figure 8: Comparison of the filter $|S_T(\omega)|^2$ for two different values of the integration time T_c.

where λ_{OPD} is OPD variation in the unitless quantity of waves (wavelengths of starlight) and the reference wavelength, λ_0, is the center wavelength of the stellar interferometer (assumed to be 550 nm).

Using Equation 13, the visibility requirement of 95% for fringe tracking or $V \geq 0.95$ corresponds to an OPD variation in waves of $\lambda_{OPD} \leq 0.05$. This becomes $\sigma_{OPD} \leq \lambda_0/20$ or $\sigma_{OPD} \leq 28\ nm\ rms$ using Equation 14. For fringe acquisition, $V \geq 0.71$ translates to a requirement of $\lambda_{OPD} \leq 0.13$ which is $\sigma_{OPD} \leq \lambda_0/7.5$ or $\sigma_{OPD} \leq 73\ nm\ rms$. We will however impose the stricter requirement of $\lambda_0/10$ (55 nm) described in an earlier section.

Summary of Performance Evaluation

Table 1 lists the performance variable and its corresponding requirement for each operating mode of the interferometer. σ_{e_T}, the fringe blur caused by the higher frequency

Table 1: Summary of operating modes, their performance variable and its corresponding requirement.

Operating Mode	Performance Variable	Requirement
Fringe Acquisition	$fringe\ blur$, σ_{e_T}	$\leq \frac{\lambda_0}{10}$ $(55\ nm\ rms)$
Fringe Tracking	$fringe\ blur$, σ_{e_T}	$\leq \frac{\lambda_0}{20}$ $(28\ nm\ rms)$

components of OPD variation, is directly compared to the requirement on OPD variation, σ_{OPD}, calculated in the previous section. Both requirements must be satisfied for successful interferometer operation.

Future Work

The performance metric defined in this memo will be used to evaluate the need for vibration isolation on SIM. Future memos will document both the results of the this analysis and the derivation of any vibration isolation requirements.

References

[1] S.W.Sirlin, A.M.San Martin, "A New Definition of Pointing Stability," JPL EM 343-1189, March 6, 1990.

[2] M.Colavita, "Visibility and Phasing," JPL IOM, August 10, 1994.

[3] G.Blackwood, T.Hyde, "Performance Definition and Control Loop Modelling for SITE," JPL IOM, September 9, 1994.

[4] J.W.Melody, "ISIS Integrated Model and RCS Thruster Disturbance Analysis," JPL IOM 3411-96-174 ITP, May 20, 1996.

[5] J.W.Melody, "SIM Wavefront Tilt Disturbance Analysis and Angle Feedforward," JPL IOM 3411-96-336 ITP, November 25, 1996.

[6] L.Jandura, "Vibration Isolation Subsystem, SIM Modeling Document," JPL Working Document, July 16, 1996, Draft version.

[7] L.Jandura, "Vibration Isolation Subsystem, Brassboard Hardware Document," JPL Working Document, May 23, 1996, Draft version.